# Enhancement of room temperature ferromagnetism in N-doped TiO2−x rutile: Correlation with the local electronic properties

**8 AUTHORS**, INCLUDING:

Y.A. Diaz Fernandez
University of Liverpool
**45** PUBLICATIONS **812** CITATIONS

SEE PROFILE

Lorenzo Malavasi
University of Pavia
**154** PUBLICATIONS **1,636** CITATIONS

SEE PROFILE

Federica Bondino
Italian National Research Council
**119** PUBLICATIONS **1,023** CITATIONS

SEE PROFILE

Luigi Sangaletti
Catholic University of the Sacred Heart
**173** PUBLICATIONS **2,144** CITATIONS

SEE PROFILE

# Enhancement of room temperature ferromagnetism in N-doped TiO$_{2-x}$ rutile: Correlation with the local electronic properties

G. Drera,[1] M. C. Mozzati,[2] P. Galinetto,[2] Y. Diaz-Fernandez,[3] L. Malavasi,[3] F. Bondino,[4] M. Malvestuto,[5] and L. Sangaletti[1,a)]

[1]*Dipartimento di Matematica e Fisica, Università Cattolica, via dei Musei 41, 25121 Brescia, Italy*
[2]*Dipartimento di Fisica "A. Volta," CNISM, Università di Pavia, Via Bassi 6, 27100 Pavia, Italy*
[3]*Dipartimento di Chimica, Università di Pavia, Via Bassi 6, 27100 Pavia, Italy*
[4]*Laboratorio TASC, IOM-CNR, S.S. 14, Km 163.5 I-34149 Basovizza, Italy*
[5]*Sincrotrone Trieste, S.S. 14 Km 163.5 Area Science Park, I-34149 Basovizza, Italy*

The magnetic and electronic properties of ferromagnetic undoped and N-doped TiO$_{2-x}$ rutile have been probed by soft x-ray spectroscopies. Upon N doping, a fivefold enhancement of the saturation magnetization is observed. Apparently, this enhancement is not related to an increase in oxygen vacancies, rather to additional in-gap states, arising from the replacement of O with N atoms in the rutile structure that can provide more favorable conditions for the onset of ferromagnetic ordering. © *2010 American Institute of Physics*. [doi:10.1063/1.3458699]

Recent findings of a weak room temperature ferromagnetism (RT-FM) in undoped TiO$_2$ samples[1–3] are posing basic questions on the origin of FM in closed shell oxides of titanium. In diluted magnetic oxides (DMOs) it is strongly believed that the defects, mostly oxygen vacancies (V$_O$), play a crucial role to induce FM (Refs. 4 and 5) since conventional ideas of magnetism (e.g., the carrier mediated exchange mechanism, widely accepted in Mn-doped III–V semiconductors[6]) are unable to account for the RT-FM. An alternative scenario for FM ordering in DMO (see, e.g., Ref. 7 and references therein) requires that the V$_O$ energy levels be sufficiently close to the host-conduction band in order to hybridize with the otherwise nonmagnetic conduction band, making the latter magnetic. But this is not the case of rutile TiO$_2$ because of its deep-gap defects states originating from V$_O$s. Although V$_O$ defects, yielding Ti$^{4+}$ reduction to Ti$^{3+}$, can already appear in undoped TiO$_2$, a large density of defects is required to establish a long-range ordering, to overcome the percolation threshold at the basis of the scenario explored by Zunger *et al.*[7] This is particularly true for TiO$_2$ where highly localized deep-gap defect orbitals lead to only a very-short-range defect-defect interaction. For very low densities of defects, these vacancies would fail to percolate through the sample, resulting in a vanishing Curie temperature. On this basis, a possible explanation for the origin of FM coupling in insulating DMO can be the inhomogeneity of V$_O$ distribution that can be high enough in limited regions to give FM coupling. The point is now to establish whether doping of rutile TiO$_2$ can create better conditions for the insurgence of FM ordering.

In this study, we show the effect of N-doping on the magnetic and electronic properties of TiO$_{2-x}$ rutile thin films. Upon N-doping an enhancement of ferromagnetic ordering in terms of remanent and saturation magnetization is achieved. By combining soft x-ray spectroscopy and magnetization measurements with ground state density functional calculations, we are able to show that, with respect to the undoped system, N doping does not add electronic states in the region where V$_O$ states are usually found, but introduces additional N-related low-lying acceptor and donor levels through O substitution with N. This ultimately reduces the band gap of rutile providing more favorable conditions for the onset of robust FM ordering in these compounds.

The thin films (about 40 nm thick) have been grown by rf sputtering a TiO$_2$ target on oriented sapphire (0001) substrates at 750 °C under a flux of pure Ar (undoped film) or an Ar–N mixture (95%–5%, N-doped film), at a pressure of $5 \times 10^{-3}$ mbar. The crystalline phase of each sample was checked by x-ray diffraction and micro-Raman spectroscopy. Static molar magnetization (M$_{mol}$) loops were collected at RT for magnetic fields (H) ranging between 0 and $\pm 2000$ Oe with a superconducting quantum interference device Quantum Design Magnetometer. Core level photoemission data were measured using an Al $K_\alpha$ source and a modified VG MkII spectrometer. Resonant photoemission spectroscopy (RESPES) and x-ray absorption spectroscopy (XAS) spectra have been collected at the BACH beamline of the Elettra synchrotron in Trieste (Italy).

Ground-state density functional theory (DFT) calculations have been carried out, based on the Perdew-Burke-Ernzerhof (PBE) parametrization of the generalized gradient approximation (GGA)[8] for the exchange-correlation functional. The projector augmented-wave[9] atom description is used, as implemented in the ABINIT (Ref. 10) code, adding semicore level to valence states. Calculations have been carried out on a rutile cell (6 atoms/cell) and a $2 \times 2 \times 2$ (48 atoms) supercell with one nitrogen atom substitutional to oxygen, corresponding to a $x \simeq 3.2\%$ doping level. The $k$-space grid was a $4 \times 4 \times 4$ Monkhorst–Pack[11] grid, and the plane-wave energy cutoff was 25 hartree. We performed a full cell relaxation with a maximum residual force on atoms fixed at $10^{-4}$ hartree/Å.

M$_{mol}$ versus H curves collected at RT with the external field H applied parallel to the thin film surface (Fig. 1) show an hysteresis cycle that mark the presence of a ferromagnetic-like ordering already at RT. For the N-doped sample, saturation is reached at about 30 emu/cm$^3$, a value
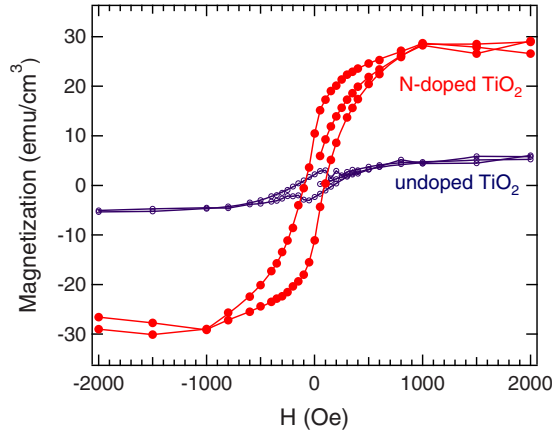
FIG. 1. (Color online) Hysteresis loop measured on the undoped TiO$_2$ (a) and on the N-doped TiO$_2$ (b) thin films. The diamagnetic contribution of the substrate, as well as that of the core electrons have been subtracted from both cycles.

much higher that the case of the undoped sample (about 5 emu/cm$^3$).

The effect of N on the electronic properties of the doped sample is discussed by examining the Ti 2$p$ and N 1$s$ core level x-ray photoelectron spectroscopy spectra of the undoped and N-doped thin films. Figure 2, left panel shows the Ti 2$p$ XPS spectrum obtained from the undoped TiO$_2$ thin film (a) and from the N-doped thin film (b). These spectra are compared with the Ti 2$p$ XPS core lines of a TiO$_2$ rutile single crystal (c). The Ti 2$p$ spectra show the typical spin-orbit split doublet of the Ti$^{4+}$ ion at a binding energy BE =458.8 eV and BE=464.8 eV. The Ti 2$p_{3/2}$ line shows a shoulder at low BE (inset of Fig. 2) that is formally assigned to a Ti$^{3+}$ oxidation state (3$d^1$ configuration).[12] This shoulder is absent in the stoichiometric TiO$_2$ single crystal surface. In the present case, it is rather important to observe that, in spite of the N-doping, the Ti$^{3+}$ component, has virtually the same weight in both samples, and therefore, we can assume that the content of 3$d^1$ magnetic ions is the same in both samples.

In the N-doped sample, the as-grown sample presents two components (N$_A$ and N$_B$) in the N 1$s$ core level region (Fig. 2, right panel). The N$_B$ peak at about BE=400 eV can be assigned either to molecular nitrogen (N$_2$) bonded to surface defects or to N bonded to surface O sites.[13,14] The in-
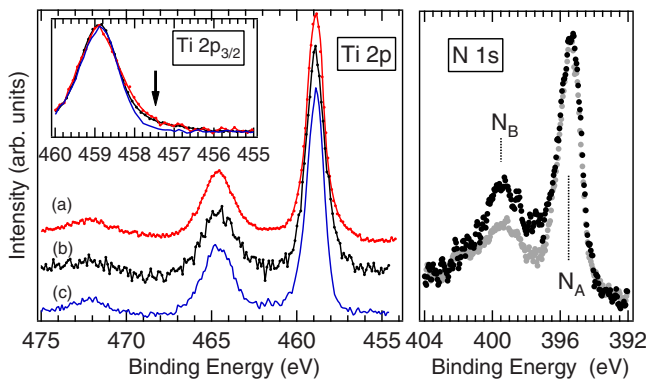


FIG. 2. (Color online) Left panel: Ti 2$p$ XPS spectrum from the undoped (a) and the N-doped (b) TiO$_2$ thin film. These spectra are compared with that collected from a stoichiometric TiO$_2$ (110) single crystal surface (c). The inset shows the Ti 2$p_{3/2}$ core line region and the vertical arrow indicates electronic states that can be ascribed to Ti$^{3+}$. Right panel: N 1$s$ photoemission spectrum at normal emission (gray dots) and at 50° off-normal emission (black dots).
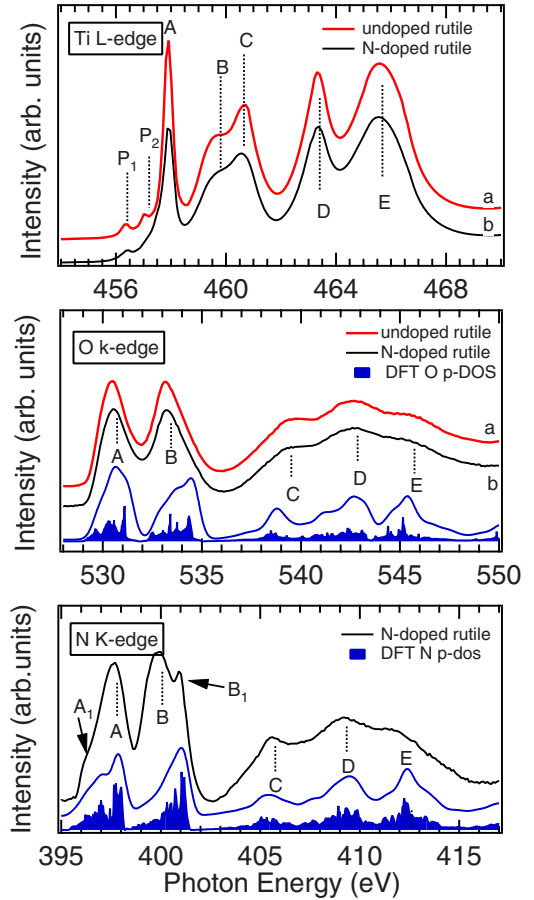


FIG. 3. (Color online) Top panel: Ti $L_{2,3}$-edge XAS spectra collected from the undoped (a) and N-doped (b) rutile thin films. Middle panel: O $K$-edge XAS spectra collected from the undoped (a) and N-doped (b) rutile thin films, compared with the undoped cell DFT calculation. Bottom panel: N $K$-edge XAS spectrum collected from the N-doped rutile thin film, compared with the supercell DFT calculations. The resolution of the monochromator was set to 0.24 eV at the Ti $L_{2,3}$-edge photon energy.

tensity of N$_B$ component increases by collecting the spectra at grazing angles, i.e., in the more surface sensitive conditions for the XPS probe, and therefore this peak is ascribed to a surface contamination. In turn, the N$_A$ peak is ascribed to bulk N atoms incorporated during the thin film growth. An estimation of the N content was carried out by considering the area of the Ti 2$p$, N 1$s$, and O 1$s$ photoemission peaks, suitably weighted by the photoemission cross section of each atomic level and the analyzer transmission. It is found that the N content in the N-doped film is about 4%.

The Ti $L_{2,3}$-edge XAS spectrum is shown in Fig. 3, top panel. This spectrum is in agreement with those already reported for rutile,[12] with a set of bands that are related to the $L_3$ edge (A, B, and C) and to the $L_2$ edge (D and E). The A and D bands are ascribed to t$_{2g}$ states arising from crystal field splitting, while the B, C, and E bands are ascribed to e$_g$ states. The P$_1$ and P$_2$ prepeaks originate from multiplet splitting for the 2$p^5$3$d^1$ final state configuration. With respect to the undoped sample, the N-doped sample shows the same energy and intensity for all peaks but a larger width. The same remarks hold also for the O $K$-edge XAS spectra (Fig. 3, middle panel). The two spectra are identical but the peaks of the N-doped sample are slightly larger than those of the undoped sample. Both spectra are well reproduced by DFT calculation of the undoped cell. Finally the N $K$-edge XAS spectrum is shown (Fig. 3, bottom panel). This spectrum is
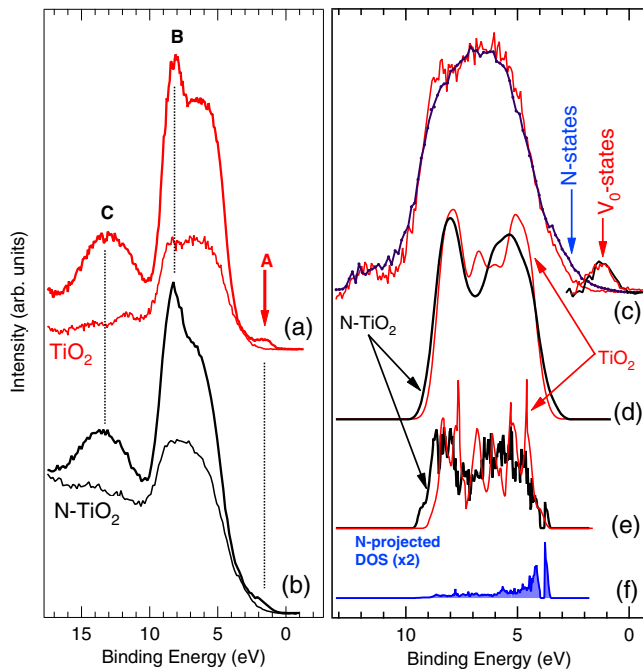
FIG. 4. (Color online) Photoemission spectra collected from the undoped (a) and N-doped (b) samples in the valence band region. Spectra drawn with a thin line have been collected with photons below the Ti $2p$-$3d$ absorption threshold ($h\nu=455$ eV), whereas spectra drawn with a thick line have been collected in resonance conditions ($h\nu=458.2$ eV). (c) Enlarged view of the off-resonance valence band spectra of the undoped (thin line) and N-doped (thick line) $TiO_2$ rutile. (d) Calculated DOS for the undoped (thin line) and doped samples (thick line) samples. (e) Convolution of the calculated DOS with a Gaussian curve (full width at half maximum=0.6 eV). (f) N-projected calculated DOS for N-$TiO_2$. The calculated DOS curves have been shifted by about $-3.5$ eV to match the measured DOS.

rather similar to that measured for oxygen, presenting a sequence of five bands (A to E). However a closer inspection shows that two additional features ($A_1$ and $B_1$) can be detected and the C, D, and E peaks appear to be shifted respect to the O $1s$ XAS spectrum. DFT supercell calculations are able to consistently reproduce most of these features. In particular, the introduction of substitutional N determines a transfer of the spectral weight toward the low photon energies in the calculated A band and toward the high photon energies in the calculated B band, consistently with the observed $A_1$ and $B_1$ experimental features. Therefore, the $A_1$ states can be regarded as N-related, donor, levels.

For a very low concentration of $V_O$s the spectroscopic signature of the electronic states can be rather elusive and therefore one has to consider also RESPES techniques to probe their existence and determine the BE. Indeed, for both samples, the study of the occupied electronic states in the valence band has been carried out with RESPES with photon energies across the Ti $L_{2,3}$-edge.

In Figs. 4(a) and 4(b), for each sample, we show the valence band photoemission spectra collected with photons below the Ti $L_{2,3}$-edge ($h\nu=450$ eV, off-resonance) and with photons corresponding to the A peak ($h\nu=458.2$ eV, on-resonance) of the Ti XAS spectrum of (Fig. 3, top panel). As can be observed, in the resonance conditions three photoemission peaks (A, B, and C) results to be enhanced. Peak C is ascribed to the Auger emission, peak B to the resonant enhancement of Ti electronic states hybridized with oxygen, and peak A to the contribution of $Ti^{3+}$ induced by $V_O$. The evidence of these in-gap states further supports the assign-

ment of the tail on the low-BE side of the Ti $2p_{3/2}$ photo-emission peak to $Ti^{3+}$ contribution. The N-doped sample shows a similar peak enhancement. The A features of both samples have been extracted by subtracting from the RESPES spectrum the off-resonance spectrum. The results are shown in Fig. 4(c) ($V_O$-states). The two peaks present identical peak energies and intensities, providing an additional proof that the vacancy-induced states contribute to both samples with equal weight.

The comparison of the off-resonance valence band spectra [Fig. 4(c)] also allows to highlight small differences in the spectral weight that are well reproduced by DFT calculations [Figs. 4(d) and 4(e)].[15] In particular, the doped sample displays a higher DOS with respect to the undoped sample for $2 \leq BE \leq 4$ eV, and below 10 eV. On the basis of the analysis of the DOS projected over the N-derived orbitals [Fig. 4(f)], the contribution at the top of the valence band, that adds electronic states (labeled as N-states) at low BE as compared to the pure rutile, is ascribed mainly to N.

In summary, we have shown that N-doping of $TiO_2$ rutile yields (i) an enhancement of ferromagnetic behavior, (ii) a replacement of about 4% O atoms in the rutile lattice with (substitutional) N atoms, and (iii) acceptor and donor levels, that determine a reduction in the rutile energy gap. This finding may have consequences on the enhancement of FM properties. In fact, the band gap reduction may favor the overlap of $V_O$ states with the empty conduction band, rendering the latter magnetic. Moreover, a highly localized deep-gap defect orbital could lead to only a very-short-range defect-defect magnetic interaction that would fail to percolate through the sample. In turn, because of the band gap reduction, the $V_O$ states can loose part of their deep-gap character and display longer-range interactions, creating more favorable conditions for the onset of magnetism (Ref. 7).

[1] S. D. Yoon, Y. Chen, A. Yang, T. L. Goodrich, X. Zuo, D. A. Arena, K. Ziemer, C. Vittoria, and V. G. Harris, J. Phys.: Condens. Matter **18**, L355 (2006).
[2] L. Sangaletti, M. C. Mozzati, P. Galinetto, C. B. Azzoni, A. Speghini, M. Bettinelli, and C. Calestani, J. Phys.: Condens. Matter **18**, 7643 (2006).
[3] N. H. Hong, J. Sakai, N. Poirot, and V. Brizé, Phys. Rev. B **73**, 132404 (2006).
[4] J. M. Coey, M. Venkatesan, and C. B. Fitzgerald, Nature Mater. **4**, 173 (2005).
[5] J. M. D. Coey, Curr. Opin. Solid State Mater. Sci. **10**, 83 (2006).
[6] A. H. MacDonald, P. Schiffer, and N. Samarth, Nature Mater. **4**, 195 (2005).
[7] J. Osorio-Guillén, S. Lany, S. V. Barabash, and A. Zunger, Phys. Rev. B **75**, 184421 (2007).
[8] J. Perdew, K. Burke, and M. Ernzerhof, Phys. Rev. Lett. **77**, 3865 (1996).
[9] M. Torrent, F. Jollet, F. Bottin, G. Zerah, and X. Gonze, Comput. Mater. Sci. **42**, 337 (2008).
[10] X. Gonze, J.-M. Beuken, R. Caracas, F. Detraux, M. Fuchs, G. -M. Rignanese, L. Sindic, M. J. Verstraete, G. Zerah, F. Jollet, M. Torrent, A. Roy, M. Mikami, Ph. Ghosez, J.-Y. Raty, and D.. C. Allan, Comput. Mat. Sci. **25**, 478 (2002).
[11] H. J. Monkhorst and J. D. Pack, Phys. Rev. B **13**, 5188 (1976).
[12] U. Diebold, Surf. Sci. Rep. **48**, 53 (2003).
[13] A. Nambu, J. Graciani, J. A. Rodriguez, Q. Wu, E. Fujita, and J. Fdez Sanz, J. Chem. Phys. **125**, 094706 (2006).
[14] S. H. Cheung, P. Nachimuthu, A. G. Joly, M. H. Engelhard, M. K. Bowman, and S. A. Chambers, Surf. Sci. **601**, 1754 (2007).
[15] The measured valence band results to be about 1 eV broader than the calculated bandwidth for undoped $TiO_2$ rutile. Quite a similar theoretical bandwidth has been recently obtained by H. M. Lawler, J. J. Rehr, F. Vila, S. D. Dalosto, E. L. Shirley, and Z. H. Levine, Phys. Rev. B **78**, 205108 (2008).